RSC Advances

ROYAL SOCIETY OF CHEMISTRY

www.rsc.org/advances

Cite this: DOI: 10.1039/c0xx00000x

www.rsc.org/xxxxxx

ARTICLE TYPE

Poly-assisted template-free synthesis novel double-shelled Co_3O_4 yolk-shell submicrospheres with excellent electrochemical properties

Yujuan Dong, Huiying Wei, Huifang Bi, Wei Liu, Wenjing Zhang, Yanzhao Yang.*

Key Laboratory for Special Functional Aggregate Materials of Education Ministry, School of Chemistry and Chemical Engineering, Shandong University, Jinan, 250100, P. R. China. Fax: +86-531-88564464; Tel: +86-531-88362988; E-mail: yzhyang@sdu.edu.cn.

Novel double-shelled Co_3O_4 yolk-shell submicrospheres were successfully synthesized via a poly-assisted template-free solvothermal method and a subsequent high heat-treating process. Before being calcined, the obtained solid spheres were amorphous and the surface of the precursors was smooth. The morphology and the phase of product were characterized by several physical analysis techniques, including Power X-ray Diffraction (XRD), Scanning Electron Microscopes (SEM) and Transmission Electron Microscopes (TEM). The LAND cell test system revealed the electrochemical properties of the final products. The as-prepared double-shelled yolk-shell submicrosphers showed a remarkable initial specific discharge capacity of about 1634mAh g^{-1}. From the 2st cycle to the 70st cycle, the discharge specific capacity of double-shelled yolk-shell submicrosphers varied from1283.2 to1091mAh g^{-1} with a retention rate of around 85.03%, corresponding to a fading rate of 2.17% per cycle. Moreover, possible growth mechanism of the yolk-shell spheres from solid spheres precursor was also proposed.

1 Introduction

Single-, double-, multiple-shelled spheres due to its potential properties are attracting increasing attention in a wide range of applications, such as catalysis,[1-2] gas sensors ,[3-4] drug delivery [5-6] and especially for energy storage of lithium-ion batteries.[7-9] The increased performance much depends on the extra space during the layer-to-layer which not only provides an opportunity to increase the contact between the electrolyte and the electrode but also shortens the diffusion distance for Li^+ insertion/extraction. Recently, various scientists and science researches try serious methods to synthesize multilayer structure. One of common methodologies is employing hard or soft templates, such as vesicles,[10] silica,[11] carbon,[12-14] metal oxide nanoparticles [14] and uniform polymers.[7] For example, Lai et al. have been prepared multiple-shell different metal oxide hollow microspheres by employing sacrificial carbonaceous templates.[13] In addition, Wang et al. have reported Co_3O_4 nanosheet-assembled multishelled hollow spheres by using PVP as the templates and showed excellent electrochemical properties.[7] However, the removal of templates easily makes the existing specific structure collapsed during the synthesis process, thus, template-free method has become a promising candidate for preparing novel special class so-called yolk-shell structures. Due to its simplicity of operation, preparing desired structure free of templates has become increasingly fascinating in recent years. Pan et al. have successfully prepared novel multiple-shell VO_2 hollow microspheres free of templates via an inside-out Ostwald-ripening and repeated Ostwald-ripening process just depending on different time duration and concentration of precursors.[8] Moreover, Hong et al. have recently synthesized double-shelled SnO_2 yolk-shell-structured powders through one-plot spray pyrolysis, a gas phase reaction method and also showed high rate capacity.[15] Therefore, synthesizing other metal oxide double-shelled or multiple-shelled yolk-shell structures through a facile template-free method should be realized and it still would be a further challenge. Nevertheless, there has been no report to introduce the free-template synthesis of single-, double- and multiple-shelled yolk-shell spheres till now.

With high theoretical capacity of ~890mA h g^{-1}, low cost and toxicity, Co_3O_4 nano/micro structures have been selected as an ideal material for anode materials of lithium ion batteries. A poly-assisted process was adopted to prepare spherical structure, in which ethylene glycol is treated as an crossing-linking.[16-17] In this study, a novel double-shelled Co_3O_4 yolk-shell submicrospheres have been successfully synthesized via a simple template-free poly-assisted process and subsequent heating-treatment from amorphous solid spheres. The products gained through different solvothermal reaction time all showed high specific capacity and excellent cycling stability. The possible formation mechanism of such novel double-shelled yolk-shell and yolk-shell spheres was also investigated.

2 Experimental

2.1 Materials

Ethylene glycol (HOC_2H_4OH, absolute for analysis) and cobalt nitrate hexahydrate ($Co(NO_3)_2{\cdot}6H_2O$) are bought without further purity

2.2 Synthesis of products

Template-free synthesis of multiple-shelled Co_3O_4 submicrospheres through a poly-assisted process under solvothermal condition followed by calcination: 2.0mmol Co $(NO_3)_2{\cdot}6H_2O$ was dissolved into 40ml $HOCH_2CH_2OH$ with stirring. Stirred for about 2h, the transparent solution was transferred into a 50 mL Teflon-lined stainless steel autoclave and

maintained at 220 ℃ for 8-24h. Notably, no deposits can be obtained when the reaction time is low for 8h at 220℃. After the autoclave was cooled naturally to room temperature, the pink samples were collected and washed by centrifugation at 10000ppm for at least three times using absolute ethanol. The as-synthesized samples were then dried in an oven in air at 80 °C to get the powders as the precursor. The precursor was then calcined to form brown powers at 500-600℃ for 2-4 hours in air.

2.3 Structural and phase characterization

Phase measurements were performed by power X-ray diffraction (XRD, Philips X'Pert Pro Super diffractometer, Cu Kα radiation λ = 1.54178). The XRD patterns were recorded from 8° to 80° at a scanning speed of 2° min^{-1}. The morphology of the prepared products was characterized by using field-emission scanning electron microscopy (FESEM, JSM-6700F, JEOL) and transmission electron microscopy (TEM, JEM-2100F operated at 200 kV).

2.4 Electrochemical characterization

Electrochemical analyses were performed using coin-type cells (CR2032). The diameter of the electrode is 12 mm, the thickness of the coating is 200μm and the density of the active material is about 1 mg cm^{-2}. Working electrodes were prepared by active materials, carbon black and polyvinylidene fluoride (PVDF) at a weight ratio of 50:30:20 onto Cu foil. Finally the well-coated foil were dried at 80℃ for 12 h in air. The electrolyte was used 1 M $LiPF_6$ mixed with ethylene carbonate (EC), dimethyl carbonate (DMC) and diethyl carbonate (DEC) in a ratio of 1:1:1 (v:v:v). The cells were assembled in an argon-filled M Braun glovebox model Unilab using airtight glass containers. The galvanostatic charge-discharge cycling measurements were performed using CT2001A LAND Cell test system.

3 Results and discussion

3.1 Phase and morphology of samples

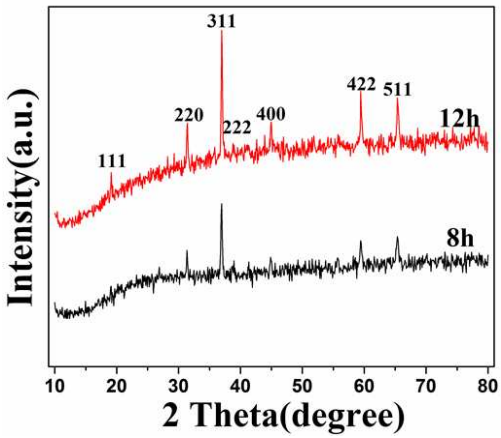

Fig. 1 XRD patterns of as-prepared Co_3O_4 multishelled spheres obtained through solvothermal process for 8h and 12h and subsequent high heating treatment in air at 600℃ for 2h.

The Co_3O_4 yolk-shell submicrospheres were gained via a poly-assisted solvothermal process at 8h and 12h (named as 8h-Co and 12h-Co) and a subsequent heating treatment. Phase and crystallinity of the samples were investigated by X-ray diffraction (XRD) as shown in Figure 1. All reflection peaks of the XRD patterns belonged to cubic spinel Co_3O_4 (JCPDS card no. 42-1467) with no impurities. [18] In addition, the identical peaks could be obtained even prolonging the reaction to 24h (see the supporting information S.1a)

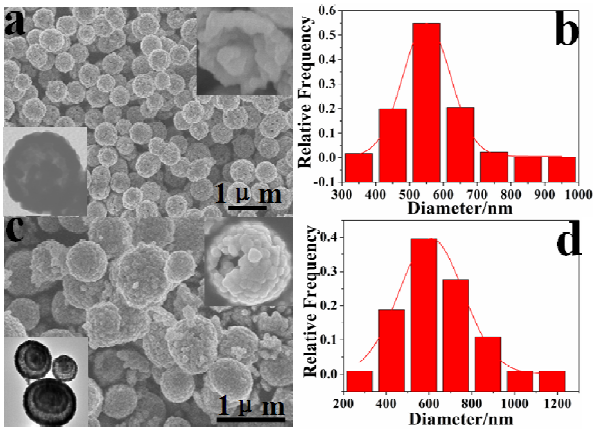

Fig. 2 FESEM image and size distribution of multiple-shelled Co_3O_4 nanospheres obtained by solvothermal process and subsequent high heating treatment in air at 600℃ for 2h, 8h(a, b); 12h(c, d)

FESEM and TEM images (Figure 2) perfectly revealed the morphology and the structure of as-prepared Co_3O_4 yolk-shell submicrospheres. When reaction time reached 8h (Fig. 2a), highly uniform Co_3O_4 yolk-shell submicrospheres were obtained, with an average diameter of about 550nm (Fig. 2b). Notably, the cracked yolk shell submicrospheres could help us observe the inner core and the outer shell clearly (insert SEM and TEM images in Fig. 2a). The insert SEM images showed that the core and the outer shell of yolk shell submicrospheres were composed of smaller ball-liked particles and the void during several balls was easily seen, corresponding to the insert TEM images in Fig 2a. When the reaction time was extended to 12h, all most submicrospheres grew into double-shelled yolk-shell structure with an average diameter of around 620nm (Figure 2d), and the cracked double-shelled submicrospheres made us observe the layers clearly. Particles and gaps were also seen in the outer shells from the insert SEM image, which were consistent with the insert HRTEM images in Fig. 2c.While the size became a little un-uniform and the insert TEM image showed a portion of triple-shelled submicrospheres. When the reaction is over 24h, the double-shell Co_3O_4 yolk-shell submicrospheres were also obtained, with an average diameter of about 780nm (Figure S1b and 1c), while some bigger spheres were obtained with the diameter were close to 1μm and the TEM images of the bigger spheres shown triple-shelled yolk-shell microspheres. Nevertheless, the outer shell of all most spheres obtained through 24h-treatment were shown some dents, may be due to excessive reaction.

To further discuss the formation of multiple-shelled submicrospheres, some researches of the precursor of the samples 8h-Co, 12h-Co and 24h-Co becomes quite necessity. As shown in Fig. S2a, 2b and 2c, the precursors were all composed of solid spheres with smooth surface and the average diameters were about 690nm, 850nm and 1.07μm (insert images of size distribution), respectively, which is highly bigger than the samples after heating-treatment. Moreover, it is worth noting that the precursors of all samples 8h-Co, 12h-Co and 24h-Co have not any typical characteristic peaks, indicating that the precursor are aggregated with amorphous particles.[19-21]

3.2 Influence factors of the formation of multiple-shelled spheres

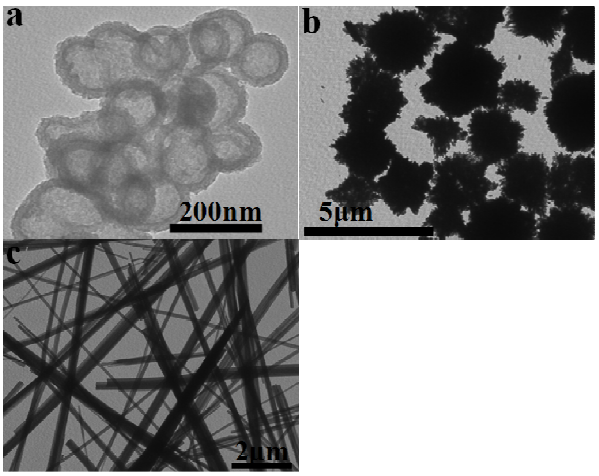

Fig. 3 TEM of precursors obtained by different material or different solvents through solvothermal reaction; a)$Co(NO_3)_2.6H_2O$+diethylene glycol; b)$Co(CH_3COO)_2 \cdot 4H_2O$+ethylene glycol; c) $Co(SO_4)_2$+ethylene glycol.

To further discuss the influence factors of the formation of multiple-shelled yolk-shell spheres, the materials and the solvent were changed respectively to do the experiment under other same condition as shown in Fig. 3. When the solvent was replaced of diethylene glycol, It is shown that hollow nanospheres could be obtained (Fig. 3a) with an average diameter of 100nm, demonstrating the polyols played a role of a cross-linking solvent. Fig. 3b and 3c showed that micro-flowers and nanowires rather than spherical objects were gained when the anion of the materials, NO_3^- were substituted by CH_3COO^- and SO_4^{2-}, respectively. Thus, the materials composed of the NO_3^- played a crucial role in the formation of solid spheres. Maybe, the successful synthesis of single-, double-, multiple-shelled spheres without templates was ascribed to the synergistic of the anion of the materials and the solvent of ethylene glycol.

3.3 Possible growth mechanism of the multiple-shelled spheres

A possible growth mechanism of such multiple-shelled yolk-shell spheres had been proposed through the following straightforward process (scheme 1). Firstly, ethylene glycol and the initial materials consisted of NO_3^- was treated at 220℃ for at least 8h via a solvothermal process to form solid spheres with smooth surface. Through subsequent calcination process, solid spheres grew into yolk-shell submicrospheres and the solvent was removed at high temperature in air, which resulted the diameters of yolk-shell spheres being shrunkened to some extent, compared to the size of their solid spheres. The successful preparation of the solid spheres was attributed to the aggregation of amorphous ball-like particles and simultaneous the link-function of ethylene glycol and then the precursors grew into yolk-shell structure during heating-treatment, which was consistent with the inset images of the TEM and SEM in Fig. 2a. Moreover, when the reaction time was over 12h, the ball-like particles re-aggregated by the link-function outside the as-synthesized

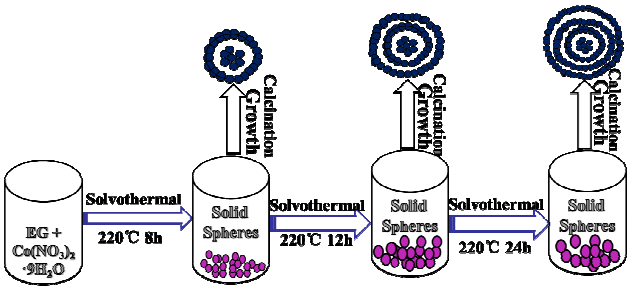

Scheme 1 Schematic illustration of the morphological evolution through poly-assisted solvothermal treatment and subsequent calcination at high temperature in air

spheres, while the re-aggregation became more and more difficult for cross-linking solvent to form double or multiple shells with an extent saturation of material at the same ambient temperature. Therefore, the size of double-shelled spheres gained through 12h-treatment was a little un-uniformity, corresponding to the image in Fig. 2c. As the reaction time was extended to 24h, a considerable number of multiple shells spheres were obtained due to the re-aggregation outside of some double-shelled spheres, thus, the uniformity of multiple-shelled spheres obtained through 24h-treatment was much worse, which could be easily seen in Fig. S1b. Finally, the removal of solvent possibly leaded to the shrunken of the spheres (size distribution in Fig. 2b, 2d and the insert images in Fig. S1a, 1b)and the formation of the void between outer layers and the gap between the inner ball-like particles (insert images in Fig. 2a and 2c) during calcination process. More importantly, the gap between layers could shorten the transport distance of ion and strengthen the potential application of lithium ion battery.

3.4 Electrochemical performance

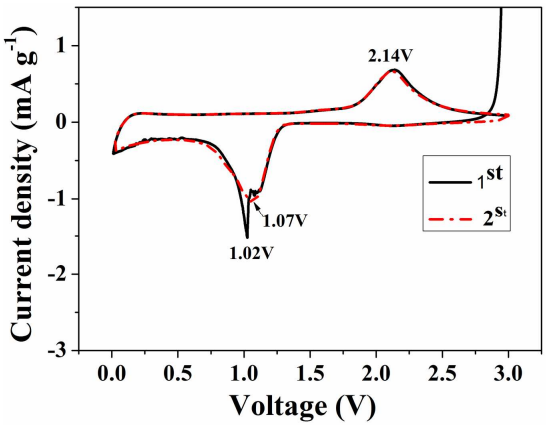

Fig.4 CV curves of the double-shelled yolk-shell spheres obtained through 12h-treatment.

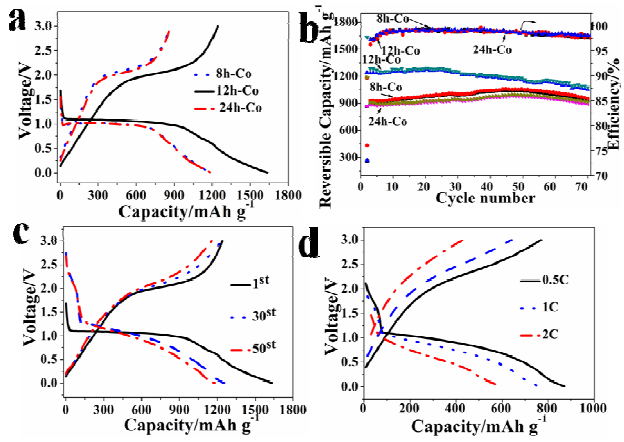

Fig. 5 Electrochemical characterization of Co_3O_4 multiple-shelled yolk-shell submicrospheres. a) The first discharge-charge curves of 8h-Co submicrospheres, 12h-Co submicrospheres, 24h-Co submicrospheres at C/5(178mAh g^{-1}). b) Cycling performance of all 12h-Co submicrospheres at C/5 (178 mAh g^{-1}). c) Discharge-charge curves of the first (—), 30th(· · ·) and 50st(- · - ·) cycles of 12h-Co submicrospherers. d) Discharge-Charge curves of 12h-Co submicrospheres at different rates.

The electrochemical behaviors of the 8h-Co, 12h-Co and 24h-Co electrode were evaluated in a potential range of 10 mV to 3V. In Fig.4, the Cyclic Voltammogram (CV) curves of 12h-Co obtained at a scan of 0.1mV/s showed the redox reaction during the charge-discharge process. In the first cycle, one sharp peak shifted at 1.02V with a small shoulder at 1.07 V in the cathodic process was assigned to the reduction of Co_3O_4 to Co. During the first anodic process, the oxidation reaction was occurred at 2.14V, indicating the formation of Co_3O_4. In the second cycle, the two reduction peaks was merged into one broad peak, while the anodic process almost without changes. The upshift of peaks was ascribed into irreversible reaction with the electrolyte and the formation of SEI layer [22-23]. Fig. 5a shows the discharge-charge curves of all three samples at a current density of 178mA g^{-1}, and the shapes of the curves are highly similar with each other. The concrete initial discharge capacities of all samples (Fig.5a) 8h-Co, 12h-Co and 24-Co were 1182.6,1634 and 1189.6mAh g^{-1}, respectively, all of which are higher than their theoretical values (890mAh g-1).[24-25] The extra specific capacity could be ascribed to the irreversible electrolyte decomposition reaction,[26-29] which easily leads to the formation of solid electrolyte interphase(SEI) layer on the surface of the electrode and increasing of the interfacial storage of lithium ion. The 12h-Co submicrospheres have higher specific capacity than the other two samples, which was ascribed to the higher void between the layers. While the lower specific capacity of 24h-Co micro-spheres was due to its size uniformity. In spite of the irreversible loss, high charge capacities of all samples 8h-Co, capacity of 12h-Co is higher than the other two samples during 70 cycles as shown in Fig. 5a. Fig. 5b shows that the capacities of 8h-Co and 24h-Co were a little lower than 12h-Co, but the tendency of the two samples are different from 12h-Co. From the 1st cycle to about the 50st cycle, the capacities of the two samples 8h-Co and 24h-Co were not reduced but aggrandized due to the insert of the electrolyte with the increase of cycling times. After 50 cycles, the capacity of the two samples 8h-Co and 24h-Co began to reduce, but the high discharge capacities of 959.8 and 920.9mAh g^{-1}still could be obtained, respectively. The same tendency has also been reported before. [32] Notably, from the 2st cycle to the 30st cycle, high capacity retention rate of 12h-Co (about 97.97%) could be attained, corresponding to a fading rate of 0.06% per cycle. After 30 cycles, the attenuation rate of 12h-Co increases gradually, but the high discharge capacities of 1252.3, 1177.8 and 1091.6mAh g^{-1} still could be obtained after 30, 50 and 70 cycles, respectively, corresponding to Coulombic Efficiency(CE) of 98.7, 98.3 and 98%(Fig. 5b and5c). More importantly, even at 0.5, 1 and 2C, the discharge specific capacities of 929.9, 796.3 and 641.6 mAh g^{-1} still could be obtained (Fig. 5d). The excellent electrochemical property is usually attributed to its unique structural features.

4 Conclusion

In summary, a template-free poly-assisted method was used to successfully prepare double-shelled or single Co_3O_4 yolk-shell submicrospheres at different reaction time. Without being heating treatment, the solid spheres were obtained with amorphous particles aggregating and the link-function of ethylene glycol. By contrast with different solvent or different materials under same other condition, the synergistic of anion of the initial materials and the solvent of ethylene glycol played a key role in forming solid spheres precursor. After high heating-treatment in air, the size of double-shelled or single Co_3O_4 yolk-shell submicrospheres showed different degree of narrowing which was ascribed to the removal of cross-linking solvent. The Co_3O_4 yolk-shell submicrospheres through 8h-solvothermal-treatment showed a first increasing and then decreasing tendency of specific discharge capacity, which was due to the insertion of the electrolyte with the increasing of cycle numbers. Moreover, the as-prepared double-shelled Co_3O_4 yolk-shell submicrospheres with12h-solvothermal-treatment displayed a high initial discharge specific capacity of 1643mAh g-1 at 178mA g^{-1}, and still kept 1177.8mAh g^{-1}after 50 cycles with a high retention of about 72.08%. Even at a rate of 2C, the specific capacity of 641.6 mAh g^{-1} was successfully gained.

5 Acknowledgements

This work was supported by the Natural Science Foundation of China (grant No. 21276142 and 21476129).

6 References

1. Cong-Min Fan, Lin-Fei Zhang, Sha-Sha Wang, Dong-Hong Wang, Li-Qiang Lu and An-Wu Xu. Nanoscale, 2012, 4, 6835–6840.
2. H. Li, Z. Bian, J. Zhu, D. Zhang, G. Li, Y. Huo, H. Li, Y. Lu, J. Am. Chem. Soc. 2007, 129, 8406-8407.
3. Lili Wang, Zheng Lou, Teng Fei and Tong Zhang.J. Mater. Chem., 2011, 21, 19331–19336.
4 X. Lai, J. Li, B. A. Korgel, Z. Dong, Z. Li, F. Su, J. Du, D. Wang, Angew. Chem. 2011.
5. J. Liu, S. Z. Qiao, S. B. Hartono, G. Q. M. Lu, Angew. Chem.2010, 122, 5101-5105.
6. M. Matsusaki, H. Ajiro, T. Kida, T. Serizawa, M. Akashi, Adv.Mater. 2012, 24, 454 457.
7. Xi Wang, Xing-Long Wu, Yu-Guo Guo, Yeteng Zhong, Xinqiang Cao,Ying Ma, and Jiannian Yao. Adv. Funct. Mater. 2010, 20, 1680–1686.

8. Anqiang Pan, Hao Bin Wu, Le Yu, and Xiong Wen (David) Lou. Angew. Chem. Int. Ed. 2013, 52, 2226-2230.
9. H. X. Yang, J. F. Qian, Z. X. Chen, X. P. Ai and Y. L. Cao, J. Phys.Chem. C, 2007, 111, 14067.
10. H. Xu, W. Wang, Angew. Chem. Int. Ed. 2007, 46, 1489.
11. J. Liu, S. B. Hartono, Y. G. Jin, Z. Li, G. Q. M. Lu, S. Z. Qiao, J. Mater. Chem. 2010, 20, 4595 4601.
12. X. Lai, J. Li, B. A. Korgel, Z. Dong, Z. Li, F. Su, J. Du, D. Wang, Angew. Chem. 2011, 123, 2790-2793.
13. Xiaoyong Lai, Jun Li, Brian A. Korgel, Zhenghong Dong, Zhenmin Li, Fabing Su, Jiang Du,and Dan Wang.Angew. Chem. Int. Ed. 2011, 50, 2738 –2741.
14. Mun Yeong Son, Young Jun Hong and Yun Chan Kang. C h e m . Com mun. 2013, **4 9**, 5678-5680.
14. X.W. Lou, C. Yuan, L. A. Archer, Adv. Mater. 2007, 19, 3328-3332.
15. Young Jun Hong , Mun Yeong Son , and Yun Chan Kang.Adv. Mater. 2013, 25, 2279–2283.
16. X. Jiang, Y. Wang, T. Herricks, Y. Xia, J. Mater. Chem. 2004, 14, 695.
17. Y. Wang, X. Jiang, Y. Xia, J. Am. Chem. Soc. 2003,125, 16 176.
18. X.W. Lou, D. Deng, J. Y. Lee, J. Feng, L. A. Archer, Adv.Mater. 2008, 20, 258-262.
19. Liang-Shu Zhong, Jin-Song Hu, An-Min Cao, Qiang Liu,Wei-Guo Song, and Li-Jun Wan. Chem. Mater., 2007 19, 1648-1655.
20. Dongping Lv, Mikhail L. Gordin, Ran Yi, Terrence Xu, Jiangxuan Song,Ying-Bing Jiang, Daiwon Choi, and Donghai Wang. *Adv. Funct. Mater.* 2014, *24*, 1059-1066.
21.Y. Sharma , N. Sharma , G. V. Subba Rao , B. V. R. Chowdari , Adv. Funct. Mater. **2007**, 17, 2855.
22. Sun, Y.; Hu, X.; Luo, W.; Huang. J. Mater. Chem. 2012, 22, 13826-13831.
23. Mohammad Akbari Garakani, Sara Abouali, Biao Zhang, Curtis Alton Takagi, Zheng-Long Xu,Jian-qiu Huang, Jiaqiang Huang, and Jang-Kyo Kim. ACS Appl. Mater. Interfaces 2014, 6, 18971-18980.
24. Wenj uan Jiang, Weiyao Zeng, Zengsheng Ma, Yong Pan, Jianguo Lin and Chunsheng Lu. RSC Adv., 2014, 4, 41281-41286.
25. Jing Bai , Xiaogang Li , Guangzeng Liu , Yitai Qian , and Shenglin Xiong.Adv. Funct. Mater. 2014, 24, 3012–3020.
26. Xi Wang, Xing-Long Wu, Yu-Guo Guo, Yeteng Zhong, Xinqiang Cao,Ying Ma, and Jiannian Yao. Adv. Funct. Mater. 2010, 20, 1680-1686.
27. H. Wang, L.-F. Cui , Y. Wang , H. S. Casalongue , J. T. Robinson, Y. Liang, Y. Cui, H. Gai, *J. Am. Chem. Soc.* 2010, *132*, 13978.
28. B. Z. Jang, C. Liu , D. Neff, Z. Yu, M. C. Wang, W. Xiong, A. Zhamu, *Nano Lett.* 2011, *11*, 3785.
29. Xin Gu, Liang Chen, Zhicheng Ju, Huayun Xu, Jian Yang and Yitai Qian. *Adv. Funct. Mater.* 2013, *23*, 4049–4056.
30. Shenglin Xiong, Jun Song Chen, Xiong Wen Lou, and Hua Chun Zeng.Adv. Funct. Mater. **2012**, 22, 861–871.